The 4th European sCO2 Conference for Energy Systems
March 23-24, 2021, Online Conference

2021-sCO2.eu-106

MEAN-LINE ANALYSIS FOR SUPERCRITICAL CO_2 CENTRIFUGAL COMPRESSORS BY USING ENTHALPY LOSS COEFFICIENTS

Haikun Ren*
University of Duisburg-Essen
Duisburg, Germany
Email: haikun.ren@uni-due.de

Alexander Hacks
University of Duisburg-Essen
Duisburg, Germany

Sebastian Schuster
University of Duisburg-Essen
Duisburg, Germany

Dieter Brillert
University of Duisburg-Essen
Duisburg, Germany

ABSTRACT

In order to develop the technology of carbon dioxide at so-called supercritical state (sCO_2)[1] further, quick and reliable design tools for the different system components, e.g. centrifugal compressors, are required. In this study, a computer program is developed to predict the performance of centrifugal compressors with sCO_2 as working fluid. This computer program is based on mean-line analysis, calculates the fluid parameters at selected sections of the meridional plane and plots the performance maps. So-called enthalpy loss coefficients are utilized to describe the difference between the isentropic and the polytropic process. In addition to previous studies, the presented model intends to predict the performance of sCO_2 centrifugal compressor with a shrouded impeller and a vaneless diffuser. For this purpose, corresponding loss coefficients are incorporated. Subsequently, the predicted results of this work are compared and validated with computational fluid dynamics (CFD) and experimental results from the EU-project sCO2-HeRo. The prediction of the computer program fits within 5% deviation to the CFD results, and about 4% to the experimental results regarding to pressure ratio.

INTRODUCTION

In recent years, sCO_2 is considered to be applied in various industrial branches such as solvent and power cycles. In the field of sCO_2 power cycles, new designs of systems and their components are required to propel the technology up to a higher technology readiness level (TRL). For this purpose, quick and reliable off-design tools for system components are needed to predict the performance characteristics of these components, especially for turbomachines of power cycle. Therefore, the so-called mean-line analysis is selected, which is widely used in the design process of turbomachines to quickly estimate and evaluate the performance of a design. By using such a method, various loss models must be taken into account, which describe the loss mechanisms of parts of the turbomachine and estimate the losses through the flow passage, in order to bring the calculation results close to reality. These loss models are already developed for example by Coppage et al. [1], Jansen [2], Johnston and Dean [3], Aungier [4]. Since many loss coefficients within these models are empirically obtained through experiments with conventional fluids like air or water, these models should be validated whether they can be utilized for CO_2.

In previous investigations, Lee et al. [5], Ameli et al. [6], and Romei et al. [7] have validated the application of conventional enthalpy loss coefficients for sCO_2 centrifugal compressors with the experimental results from Sandia National Laboratories (SNL) [8]. Similarly, Cho et al. [9] have investigated different sets of loss coefficients referred by Oh et al. [10], Galvas [11], and Lee et al. [12] and validated them with the experimental results from Korea Advanced Institute of Science and Technology (KAIST) and Korea Atomic Energy Research Institute (KAERI). The results from these investigations exhibit a good agreement with the experimental results in tendency. In addition to previous works, different configuration of centrifugal

[1] sCO_2 is defined as carbon dioxide at supercritical state, namely $p > p_{crit}$ and $T > T_{crit}$. The critical pressure p_{crit} and temperature T_{crit} of CO_2 are 73.75 bar and 304.13 K respectively.

* corresponding author(s)

DOI: 10.17185/duepublico/73948

compressor is considered in this work. The main contribution of this study is that the results of this work are validated quantitatively with the results from EU-project sCO2-HeRo.

In this study, a computer program is established in MATLAB by utilizing the mean-line analysis and enthalpy loss coefficients in order to predict the performance of sCO_2 centrifugal compressor quickly within an acceptable deviation. This computer program is validated with the CFD and experimental results from sCO2-HeRo, in which a shrouded 2D impeller and a vaneless diffuser are employed. Additionally, the computer program also considers parasitic works for validation with experiments, since they increase the input power of the compressor.

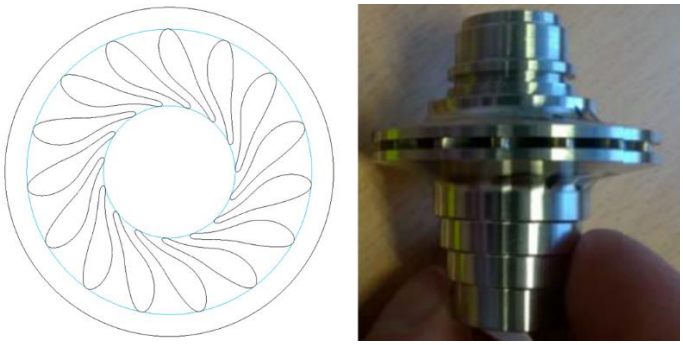

Figure 1: Compressor wheels of CO2-HeRo [13]

MEAN-LINE ANALYSIS

In order to calculate the flow properties through a centrifugal compressor with mean-line analysis, sections are defined in Figure 2. According to this definition, 1-2 is the impeller, 3-4 is the diffuser, 4-5 is the volute, and 5-6 is the exit cone. Obviously, section 1 is the inlet and section 6 is the outlet of the compressor.

Especially for centrifugal compressors, parasitic works due to recirculation and disk friction must be considered, see Figure 2. The recirculation work is caused by swirl due to the backflow from diffuser to the impeller tip, normally found at low flow coefficient [4]. The disk friction, which is caused by the frictional force on the both side of the impeller exerted by the leakage flows in the clearance between impeller outer surface and the casing, builds torque against the direction of rotation and therefore causes an additional work [4]. These mechanisms lead to an additional power consumption to the shaft, which means an additional torque M_a on the shaft. Denoted the specific blade work by a, the total power consumption at the shaft is

$$P_t = \dot{m} \cdot a + \omega \cdot M_a, \tag{1}$$

with

$$a = u_2 c_{u2} - u_1 c_{u1}, \tag{2}$$

where $\dot{m}$ is the mass flow rate through the impeller and ω the angular velocity of the impeller. u and c_u represent the circumferential velocity and the circumferential component of the absolute velocity. 1 and 2 are the section number.

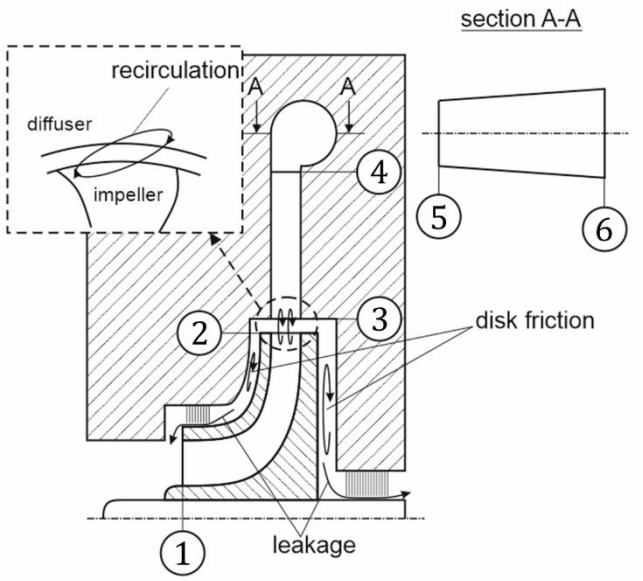

Figure 2: Meridional plane of a centrifugal compressor with defined sections and mechanisms of parasitic works

Since the recirculation is found inside the main flow passage and causes an energy dissipation, the recirculation work contributes a specific total enthalpy rise $L_{t,rc}$ to the main flow corresponding to this dissipation. Similarly, the disk friction at the impeller shroud side impacts the flow within the impeller due to the backflow from impeller tip to impeller inlet. Therefore, this part of disk friction work also leads to a specific total enthalpy rise $L_{t,df}$ which is corresponding to an energy dissipation. Although the disk friction on the both sides of the impeller contribute to the additional torque M_a in eq.(1), the disk friction on the impeller does not contribute to the energy dissipation of the main flow in an adiabatic system. Finally, a total specific enthalpy rise[2] $L_{t,p}$ due to the parasitic works beside the specific blade work a is given by

$$L_{t,p} = L_{t,rc} + L_{t,df}. \tag{3}$$

By estimating the circumferential component c_{u2}, the specific total enthalpy at the impeller outlet is calculated by the first law of thermodynamics for adiabatic flows:

$$h_{t2} = h_{t1} + a + L_{t,p}, \tag{4}$$

in which t represents parameters respect to total thermodynamic conditions. Thereafter, the losses are considered and the total pressure p_{t2} at impeller outlet is calculated. This is achieved by taking into account the difference between the specific total enthalpy at impeller outlet h_{t2} for the polytropic and $h_{t2,is}$ for the isentropic process, and by calculating $h_{t2,is}$ as

[2] The equations of $L_{t,rc}$ and $L_{t,df}$ are found in the annex.

$$h_{t2,is} = h_{t2} - L_{t,p} - L_{12}, \quad (5)$$

where L_{12} is the energy dissipation of the flow within the impeller, while $L_{t,p}$ is corresponding to the energy dissipation outside the impeller, as mentioned before. Finally, p_{t2} is calculated by $p_{t2} = p(h_{t2,is}, s_1)$ and other total fluid properties are calculated from the equation of state presented by Span and Wagner [14] and incorporated in NIST Refprop v8.0 [15] as $f(h_{t2}, p_{t2})$. Calculating the specific static enthalpy by $h_2 = h_{t2} - c_2^2/2$, all static fluid properties are known from the equation of state $f(h_2, s_2)$.

Afterward, the meridional component c_{m2} of the absolute flow velocity is calculated from the continuity equation, while the circumferential component is calculate by

$$c_{u2} = u_2 \cdot \left(1 + \frac{c_{m2}}{u_2} \cdot cot\beta_2\right), \quad (6)$$

where β_2 is the prescribed relative flow angle[3] at impeller outlet. Finally, the circumferential component c_{u2} is updated in an iterative process.

Similar steps apply to all other sections but with constant total specific enthalpy, which is equal to h_{t2}.

After calculating fluid parameters of all sections (1-6), the efficiency can be calculated using a desired definition. It does not impact the calculation of the thermodynamic parameters. This definition is provided in section "validation with CFD-simulations of sCO2-HeRo".

ENTHALPY LOSS COEFFICIENTS

In this study, enthalpy loss coefficients ζ are used to quantify the aerodynamic losses within the impeller and are defined as:

$$\zeta_{i(i+1)} = \frac{L_{i(i+1)}}{\frac{1}{2}c_{i+1}^2} = \frac{h_{t(i+1)} - h_{t(i+1),is}}{\frac{1}{2}c_{i+1}^2}. \quad (7)$$

Only for the impeller, the relative velocity w is used instead of the absolute velocity c, and the specific total enthalpy rise $L_{t,p}$ caused by the parasitic works outside the impeller should be subtracted, as shown in eq.(5). Hence, there is

$$\zeta_{12} = \frac{L_{12}}{\frac{1}{2}w_2^2} = \frac{h_{t2} - L_{t,p} - h_{t2,is}}{\frac{1}{2}w_2^2}. \quad (8)$$

Finally, the loss coefficient for each part of the compressor can be calculated by

$$\zeta_{12} = \zeta_{inc} + \zeta_{bld} + \zeta_{sf} + \zeta_{mix}, \quad (9)$$

$$\zeta_{34} = \zeta_{vld}, \quad (10)$$

$$\zeta_{45} = \zeta_{vol}, \quad (11)$$

$$\zeta_{56} = \zeta_{exit}. \quad (12)$$

Details about the loss coefficients applied in the equations above are listed in the annex (Table 2).

VALIDATION WITH CFD-SIMULATIONS OF SCO2-HERO

To validate the computer program, the compressor performance of sCO2-HeRo is predicted and firstly compared with the CFD results according to [16], in which the CFD results are shifted by constant value of 0.1 kg/s to lower mass flow to account for the eye seal leakage. In this paper, the original CFD results are applied. Table 1 displays parameters used to calculate the compressor performance. Several parameters such as β_2, B_1 and B_2 are derived from the CFD results, since the blade metal angle and blade contour do not reflect the actual flow parameters due to the thick blade profile shown in Figure 1. The diameter and the height of the vaneless diffuser inlet are regarded as same as those of the impeller outlet. In this case, parasitic works $L_{t,p}$ are not considered, since the CFD results do not include them.

Table 1: Parameters of the sCO2-HeRo compressor [13]

Parameter	Symbol	Value	Unit
Total pressure	p_{t1}	78.3	bar
Total temperature	T_{t1}	306.15	K
Impeller tip diameter	d_2	38.2	mm
Impeller hub diameter	d_{1h}	17.8	mm
Impeller shroud diameter	d_{1s}	17.8	mm
Impeller blade number	z_{La}	15	–
Impeller outlet flow angle	β_2	147.2	°
Impeller inlet metal angle	$\beta_{1,bl}$	157.6	°
Impeller inlet blade height	b_1	2.1	mm
Impeller tip blade height	b_2	1.25	mm
Area blockage at impeller inlet	B_1	0.16	–
Area blockage at impeller outlet	B_2	0.32	–
Diffuser outlet diameter	d_4	84	mm
Volute outlet radius	r_{vol}	3.75	mm
Exit cone outlet radius	r_{exit}	7.9	mm

In Figure 3, predicted ratio of total pressures at selected rotational speeds (20 krpm, 30 krpm, 40 krpm, and 50 krpm) are compared with the CFD results. They are calculated by

$$\Pi_t = \frac{p_{t6}}{p_{t1}}. \quad (13)$$

For the calculation of the total parameters, the flow velocity at compressor outlet is neglected corresponding to the CFD results. The mean-line results are represented by lines, while the CFD results are displayed in symbols. At all selected rotational speeds, the mean-line results are in agreement with the CFD results. Quantitatively, a maximal deviation of 3.2% is found, which exhibits a very good quality of the prediction in this case. Similarly, regarding to the increase of the isentropic specific total

[3] The flow angles are illustrated by Figure 10 in annex.

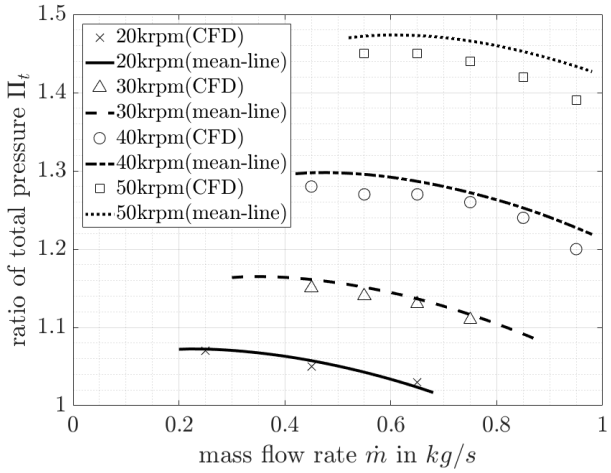

Figure 3: Comparison of ratio of total pressures between CFD and mean-line results for the compressor of sCO2-HeRo

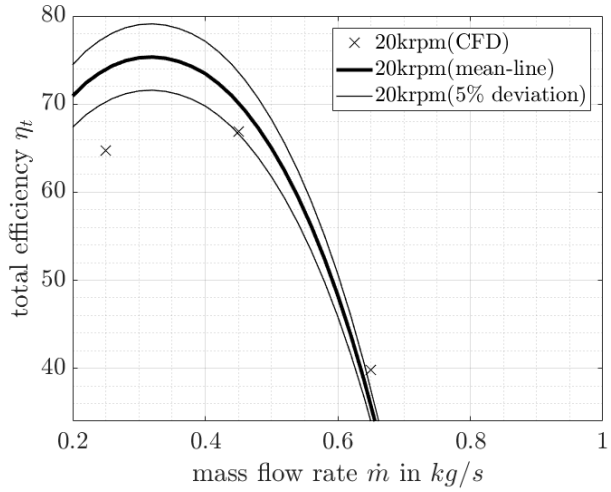

Figure 4: Comparison of efficiency between CFD and mean-line results for the compressor of sCO2-HeRo at 20 krpm

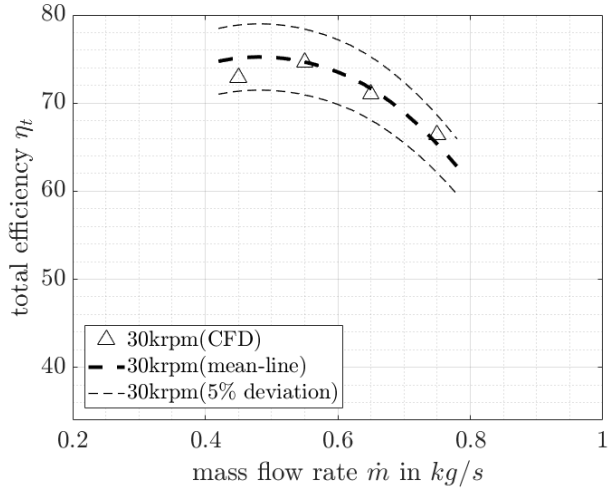

Figure 5: Comparison of efficiency between CFD and mean-line results for the compressor of sCO2-HeRo at 30 krpm

enthalpy $\Delta h_{t,is}$, 77.8% of the cases are found within the 5% deviation region.

Furthermore, the efficiency of compressor are calculated by

$$\eta_t = \frac{\Delta h_{16,is} + (c_6^2 - c_1^2)/2}{a}, \tag{14}$$

where $\Delta h_{16,is}$ is the isentropic specific enthalpy change regarding to process 1 to 6. They are compared with the CFD results as well, see Figure 5 to Figure 7. In each diagram, the broad line represents the mean-line results, while the CFD results are marked by symbols. There are two narrower lines which present a 5% deviation to the mean-line results, to distinguish the difference between mean-line and CFD results quantitatively. The comparisons exhibit that the CFD results are found within the 5% deviation range in 83.3% of the cases, which indicates that the quality of the prediction is already good with regard to the efficiency.

Consequently, the computer program is considered as

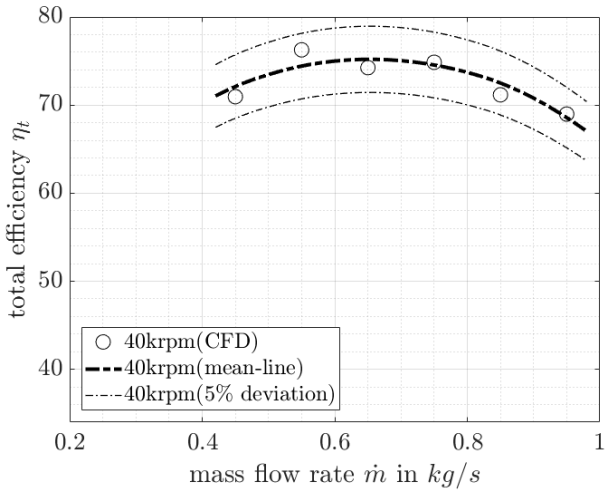

Figure 6: Comparison of efficiency between CFD and mean-line results for the compressor of sCO2-HeRo at 40 krpm

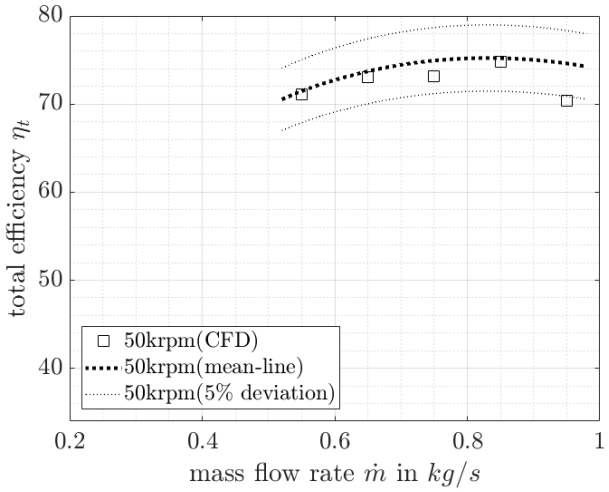

Figure 7: Comparison of efficiency between CFD and mean-line results for the compressor of sCO2-HeRo at 50 krpm

verified with the CFD results of sCO2-HeRo through the comparisons regarding to the ratio of total pressures and to the efficiency of compressor. It is specified that the prediction has an accuracy of 95% and indicates that the enthalpy loss coefficients employed in this computer program with corresponding configurations are appropriate.

VALIDATION WITH EXPERIMENTS OF SCO2-HERO

In addition, the computer program is also validated with the experimental results of sCO2-HeRo, which have been obtained in the SUSEN CO_2-loop at CVR Research Center Řež [17]. In this paper, only the pressure ratios from the experiments are presented, since the enthalpy rise and efficiency of the compressor are not determined precisely enough due to the measurement uncertainties in the experiments [16]. For the validation with experimental data, the parasitic works $L_{t,p}$, which lead to an additional specific total enthalpy rise beside the specific blade work a, are calculated by eq.(3). The leakage flows are considered as well and calculated by eq.(34) displayed in annex. For the calculation of the total parameters, the flow velocity at compressor outlet is neglected corresponding to the EXP results.

In Figure 8, the diagram illustrates the comparison between the mean-line results and the experimental results at rotational speeds of 20 krpm and 30 krpm. The experimental results are the same as in [16], displayed with symbols and error bars, and are denoted by EXP. The mean-line results are shown by lines. Graphically, the mean-line results correspond to the experimental results well in tendency. It is found that the experimental results have a maximal deviation of 3.9% to the mean-line results. This also indicates a high quality of the prediction. The computer program is hence regarded as validated with the experimental results of sCO2-HeRo in terms of the pressure ratio.

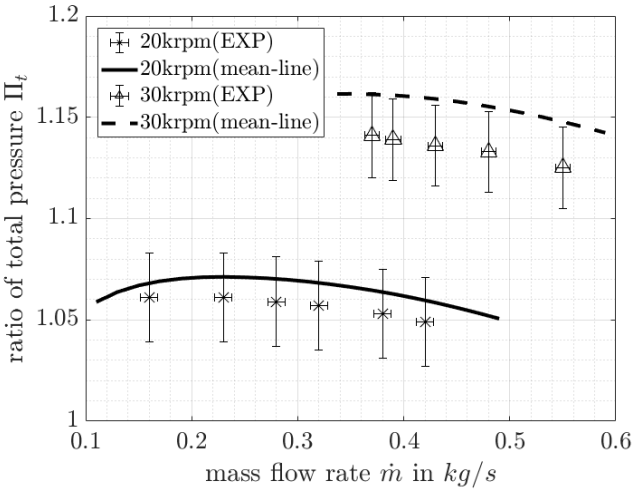

Figure 8: Comparison of the ratio of total pressures between EXP and mean-line results for the compressor of sCO2-HeRo

CONCLUSIONS

In this study, a computer program based on mean-line analysis has been established for predicting the performance especially of sCO_2 centrifugal compressors. Corresponding loss coefficients are employed to fit compressor configurations like:

- Shrouded impeller,
- 2D blades,
- Vaneless diffuser.

The parasitic works and their effects are introduced in this paper as well. In this study, the parasitic works are only incorporated into the computer program by the validation with the experimental results.

In this paper, the impeller outlet flow angle from CFD data is used in the mean-line calculation, since no deviation model is available for this geometry. Similarly, the impeller inlet and outlet area blockage are also derived from CFD data. However, the program can easily be extended with deviations and blockage models, e.g., the models mentioned by Aungier [4]. The selection of suitable models impacts the accuracy of the program.

Consequently, the computer program is validated with the results of sCO2-HeRo. The mean-line calculations fit the CFD results within a deviation of 3.2% and 5% regarding to pressure ratio and efficiency respectively. The comparison between the mean-line and experimental results of sCO2-HeRo shows a fitting within 3.9% in terms of pressure ratio.

This computer program can be used later to support the design of sCO2 centrifugal compressors with the configuration, which are validated in this study, by quickly predicting the performance.

NOMENCLATURE

Variables

a	Specific blade work (J/kg)
A	Area (m^2)
b	Blade height (m)
B	Area blockage $(-)$
c	Absolute velocity (m/s)
c_f	Skin friction coefficient $(-)$
C_M	Torque coefficient $(-)$
C_{Mr}	Torque coefficient for fully rough disk$(-)$
C_{Ms}	Torque coefficient for smooth disk$(-)$
D_f	Diffusion factor $(-)$
e	Peak-to-valley surface roughness (μm)
h	Static specific enthalpy (J/kg)
l_B	Flow passage length (m)
L	Specific loss / work (J/kg)
K	Clearance gap swirl parameter $(-)$
K_{sf}	Skin friction constant $(-)$
$\dot{m}$	Mass flow rate (kg/s)
M_a	Additional torque on the shaft (Nm)
p	Static pressure (Pa)
P_t	Power consumption at the shaft (W)

r	Radius (m)
Re	Reynolds number $(-)$
Re_r	Reynolds number, where disk becomes fully rough $(-)$
Re_s	Reynolds number, where roughness effects first appear $(-)$
s	Entropy $(\mathrm{J/(kgK)})$
t	Disk/housing gap width (m)
T	Static temperature (K)
u	Circumferential velocity $(\mathrm{m/s})$
w	Relative velocity $(\mathrm{m/s})$
z	Blade number $(-)$

Greek symbols

α	Absolute flow angle respect to the circumferential velocity (°)
β	Relative flow angle respect to the circumferential velocity (°)
ε	Seal coefficient $(-)$
ϵ	Wake area fraction $(-)$
ζ	Enthalpy loss coefficienct $(-)$
η	Efficiency $(-)$
μ	Dynamic viscosity $(\mathrm{kg/(ms)})$
Π	Pressure ratio $(-)$
ρ	Density $(\mathrm{kg/m^3})$
$\bar{\rho}$	Mean density $(\mathrm{kg/m^3})$
ω	Angular velocity $(\mathrm{rad/s})$

Subscripts

AVE	Averaged
bl	Blade parameter
bld	Blade loading
df	Disc friction
$exit$	Exit of compressor
h	Hub parameter
i	Section number
in	Inlet parameter
inc	Incidence
is	Isentropic parameter
lk	Leakage
La	Impeller parameter
m	Meridional parameter
mix	Wake mixing
out	Outlet parameter
p	Parasitic works
rc	Recirculation
rms	Root mean square
s	Shroud parameter
sf	Skin friction
t	Total thermodynamic parameter
u	Circumferential component
vld	Vaneless diffuser
vol	Volute parameter
$1-6$	Section number
12	Process from section 1 to 2

Abbreviations

CO_2	Carbon Dioxide
KAERI	Korea Atomic Energy Research Institute
KAIST	Korea Advanced Institute of Science and Technology
sCO2-HeRo	sCO2-HeRo.eu project
SNL	Sandia National Laboratories
sCO_2	Carbon Dioxide at so-called supercritical state
TRL	Technology Readiness Level
2D	Two dimensional
3D	Three dimensional

ACKNOWLEDGEMENTS

This project has received funding from the Euratom research and training programme 2014-2018 under grant agreement No 847606.

REFERENCES

[1] Coppage, J. E.; Dallenbach, F.; Eichenberger, H. P.; Hlavaka, G. E.; Knoernschild, E. M.; Van Le, N. (1956). Study of supersonic radial compressors for refrigeration and pressurization systems. AiResearch Manufacturing Company, California.

[2] Jansen, W. (1967). A method for calculating the flow in a centrifugal impeller when entropy gradients are present. Conference on Internal Aerodynamics, Cambridge.

[3] Johnston, J. P.; Dean Jr., R. C. (1966). Losses in Vaneless Diffusers of Centrifugal Compressors and Pumps: Analysis, Experiment, and Design. Journal of Engineering for Power, 49-60, ASME.

[4] Aungier, Ronald H. (1999). Centrifugal Compressors: A Strategy for Aerodynamic Design and Analysis. The ASME, New York.

[5] Lee, J.; Lee, J. I.; Yoon, H. J.; Cha, J. E. (2014). Supercritical Carbon Dioxide turbomachinery design for water-cooled Small Modular Reactor application. Nuclear Engineering and Design, Vol. 270, 76-89.

[6] Ameli, A.; Afzalifar, A.; Turunen-Saaresti, T.; Backman, J. (2019). Centrifugal Compressor Design for Near-Critical Point Applications. Journal of Engineering for Gas Turbines and Power, Vol. 141 / 031016, ASME.

[7] Romei, A.; Gaetani, P.; Giostri, A.; Persico, G. (2020). The Role of Turbomachinery Performance in the Optimization of Supercritical Carbon Dioxide Power Systems. ASME, Journal of Turbomachinery, Vol. 142 / 071001.

[8] Wright, S. A.; Radel, R. F.; Vernon, M. E.; Rochau, G. E.; Pickard, P. S. (2010). Operation and Analysis of a Supercritical CO_2 Brayton Cycle. Sandia Report SAND2010-0171, Sandia National Laboratories.

[9] Cho, S. K.; Son, S.; Lee, J.; Lee, S.; Jeong, Y.; Oh, B. S.; Lee, J. I. (2020). Optimum loss models for performance prediction of supercritical CO_2 centrifugal compressor. Applied Thermal Engineering, 28 October 2020, 116255.

[10] Oh, H. W.; Yoon, E. S.; Chung, M. K. (1997). An optimum set of loss models for performance prediction of centrifugal compressors. Journal of Power and Energy, Vol. 211, No. 4, 331-338, IMechE.
[11] Galvas, M. R. (1973). FORTRAN program for predicting off-design performance of centrifugal compressors. NASA TN D-7487, Lewis Research Center and U.S. Army Air Mobility R&D Laboratory, Cleveland, Obio.
[12] Lee, J. (2016). Study of improved design methodology of S-CO_2 power cycle compressor for the next generation nuclear system application, Ph.D. dissertation, Korea Advanced Institute of Science and Technology.
[13] Hacks, A.; Schuster, S.; Dohmen, H. J.; Benra, F.-K.; Brillert, D. (2018). Turbomachine design for supercritical carbon dioxide within the sCO2-HeRo.eu. ASME, Journal of Engineering for Gas Turbines and Power, Vol. 140 / 121017.
[14] Span, R.; Wagner, W. (1996). A New Equation of State for Carbon Dioxide Covering the Fluid Region from the Triple-Point Temperature to 1100K at Pressures up to 800 MPa. Journal of Physical and Chemical Reference Data 25, 1509.
[15] Lemmon, E. W.; Huber, M. L.; McLinden, M. O. (2007). NIST Reference Fluid Thermodynamic and Transport Properties – REFPROP, Version 8.0, User's Guide. Physical and Chemical Properties Division, National Institute of Standards and Technology.
[16] Hacks, A.; Vojacek, A.; Dohmen, H. J.; Brillert, D. (2018). Experimental investigation of the sCO2-HeRo Compressor. 2nd European supercritical CO2 Conference, Essen, Germany.
[17] Hacks, A.; Schuster, S.; Brillert, D. (2019). Stabilizing Effects of Supercritical CO_2 Fluid Properties on Compressor Operation. Int. J. Turbomach. Propuls. Power 2019, Vol. 4(3), 20.
[18] Jiang, W.; Khan, J.; Dougal, R. A. (2006). Dynamic centrifugal compressor model for system simulation. Journal of Power Sources 158, 1333-1343, Elsevier.
[19] Galerkin, Y. B.; Rekstin, A. F.; Solovyeva, O. A. (2019). Vaneless diffuser of the centrifugal compressor stage design method. AIP Conderence Proceedings 2141, 030007.
[20] Botha, B. W.; Moolman, A. (2005). Determining the Impact of the Different Losses on Centrifugal Compressor Design. R & D Journal, 21 (3), 23-31.
[21] Daily, J. W. and Nece, R. E. (1960). Chamber Dimension Effects on Induced Flow and Friction Resistance of Enclosed Rotating Disks. Transactions ASME, Journal of Basic Engineering, Sep., 553-562.
[22] Daily, J. W. and Nece, R. E. (1960). Roughness Effects on Fictional Resistance of Enclosed Rotating Disks. Transactions ASME, Journal of Basic Engineering, Mar., 217-232.
[23] Lüdtke, K. H. (2004). Process centrifugal compressors: basics, function, operation, design, application. Springer Science & Business Media. K. H.

ANNEX

ENTHALPY LOSS COEFFICIENTS

All enthalpy loss coefficients used in this study are listed in Table 2.

The wake area fraction required to calculate the mixing losses is calculated according to Botha et al. [18]. It varies linearly with the mass flow rate and takes a value of 0.5 at the surge line as well as the choke line, and 0.366 at the design point ($\zeta_{inc} \approx 0$).

The calculation of the skin friction factor c_f is corresponding to the method described by Aungier [4]. Since the blade metal angle at the impeller outlet does not fit the actual flow parameters, the value of $\beta_{2,bl}$ in eq. (17) is substituted by β_2 shown in Table 1.

Equation (21) is derived from the total pressure loss coefficient introduced in [4], by neglecting the density change in the exit cone, since the density change is small in the exit cone.

Table 2: Enthalpy loss coefficients for various loss mechanisms

Incidence loss [18]:	$\zeta_{inc} = \left(\frac{u_1}{w_2} + \frac{c_{m1}}{w_2} \cdot cot\beta_{1,bl}\right)^2$	(15)
Blade loading loss [1]:	$\zeta_{bld} = 0.1 \cdot D_f^2 \cdot \left(\frac{u_2}{w_2}\right)^2$	(16)
Skin friction loss [1,11]:	$\zeta_{sf} = 2 \cdot K_{sf} \cdot c_f \cdot \frac{\left(\frac{l_{B,La}}{d_2}\right)}{\left(\frac{d_{H,La}}{d_2}\right)} \cdot \left(\frac{w}{u_2}\right)^2_{AVE} \cdot \left(\frac{u_2}{w_2}\right)^2$	(17)
	$K_{sf} = \begin{cases} 5.6 & impller\ without\ splitters \\ 7 & impller\ with\ splitters \end{cases}$	
	$\left(\frac{l_{B,La}}{d_2}\right) = \frac{r_2 - r_{1,rms}}{d_2 \cdot sin\beta_{2,bl}} \qquad acc.to\ [1]$	
	$\left(\frac{d_{H,La}}{d_2}\right) = \frac{1}{\frac{z_{La}}{\pi sin\beta_{2,bl}} + \frac{d_2}{b_2}} + \frac{\frac{d_{1s}}{d_2}}{\frac{2}{1-\frac{d_{1h}}{d_{1s}}} + \frac{2z_{La}}{\pi\left(1+\frac{d_{1h}}{d_{1s}}\right)} \sqrt{1 + \left[1 + \frac{\left(\frac{d_{1h}}{d_{1s}}\right)^2}{2}\right] \cdot cot^2\beta_{1s,bl}}}$	
	$\left(\frac{w}{u_2}\right)^2_{AVE} = 0.5\left\{\left(\frac{c_{m1}}{u_2}\right)^2 + \left(\frac{d_{1,rms}}{d_2}\right)^2 + \left(\frac{w_2}{w_{1s}}\right)^2 \left[\left(\frac{c_{m1}}{u_2}\right)^2 + \left(\frac{d_{1s}}{d_2}\right)^2\right]\right\}$	
Mixing loss [3,10,20]:	$\zeta_{mix} = \left(\frac{c_{m2}}{w_2}\right)^2 \left(\frac{1 - \epsilon - \frac{b_3}{b_2}}{1 - \epsilon}\right)^2$	(18)
	$\epsilon = 0.5 \sim 0.366$	
Vaneless diffuser loss [19]:	$\zeta_{vld} = \frac{c_f}{4 \cdot \frac{b_3}{d_3} \cdot sin\alpha_3} \cdot \left(1 - \frac{d_3}{d_4}\right) \cdot \left(\frac{c_3}{c_4}\right)^2$	(19)
Volute loss [4,7]:	$\zeta_{vol} = \left(\frac{c_{m4}}{c_5}\right)^2$	(20)
Exit cone loss [4]:	$\zeta_{exit} = \left(\frac{c_5 - c_6}{c_6}\right)^2$	(21)

PARASITIC WORKS:

The parasitic works summarize losses due to recirculation and disk friction, which are described below. After estimating all the parasitic works, the specific total enthalpy rise due to the specific parasitic works is calculated by eq.(3).

Recirculation work:

According to Oh et al. [10], the specific total enthalpy rise due to the recirculation work can be calculated as:

$$L_{t,rc} = 8 \cdot 10^{-5} \cdot \sinh\left[3.5\left(\frac{\pi}{2} - \alpha_2\right)^3\right] \cdot D_f^2 \cdot u_2^2, \tag{22}$$

where α_2 is the absolute flow angle at impeller outlet given in radian. D_f is called diffusion factor and is given by

$$D_f = 1 - \frac{w_2}{w_{1s}} + \frac{0.75(a/u_2^2)}{\frac{w_{1s}}{w_2}\left[\frac{z_{La}}{\pi}\left(1 - \frac{d_{1s}}{d_2}\right) + 2\frac{d_{1s}}{d_2}\right]}. \tag{23}$$

In eq. (23), w is the relative flow velocity, d the diameter, and z_{La} the blade number of the impeller. The index s represents hereon the parameter in terms of shroud side.

Disk friction work:

The specific total enthalpy rise due to the disk friction work is estimated with the torque coefficient C_M according to Daily and Nece [21, 22], which is expressed by

$$C_{M1} = \frac{2\pi}{(t/r)Re} \tag{24}$$

$$C_{M2} = \frac{3.7(t/r)^{0.1}}{\sqrt{Re}} \tag{25}$$

$$C_{M3} = \frac{0.08}{(t/r)^{1/6}Re^{1/4}} \tag{26}$$

$$C_{M4} = \frac{0.102(t/r)^{0.1}}{Re^{0.2}} \tag{27}$$

with

$$Re = \frac{\rho_2 \omega r_2^2}{\mu_2}, \tag{28}$$

where t is the clearance gap width between the disk and housing, r the radius, Re the Reynolds number of the disk, ρ the density, and μ the dynamic viscosity. The torque coefficient for smooth disk surface C_{Ms} is equal to the maximum of eq.(24) to eq.(27). The surface roughness first affects the torque coefficient at the Reynolds number Re equal to Re_s which is calculated by [22]

$$Re_s = 1100(e/r)^{-0.4}/\sqrt{C_{Ms}}, \tag{29}$$

where e is the peak-to-valley surface roughness height. The Reynolds number at a fully rough disk is calculated by [22]

$$Re_r = 1100(r/e) - 6 \cdot 10^6, \tag{30}$$

while the torque coefficient C_{Mr} for the fully rough disk is written as

$$C_{Mr} = \left(\frac{1}{3.8log_{10}(r/e) - 2.4(s/r)^{0.25}}\right)^2. \tag{31}$$

The final torque coefficient C_M is calculated by

$$C_M = \begin{cases} C_{Ms} & Re \le Re_s \\ C_{Ms} + (C_{Mr} - C_{Ms}) \cdot \dfrac{log_{10}\left(\frac{Re}{Re_s}\right)}{log_{10}\left(\frac{Re_r}{Re_s}\right)} & Re_s < Re < Re_r. \\ C_{Mr} & Re \ge Re_s \end{cases} \tag{32}$$

Since this torque coefficient considers both side of the disk, the specific enthalpy rise due to the disk friction at the impeller shroud side is finally calculated by

$$L_{t,df} = C_M \cdot \frac{\rho_2 \omega^3 r_2^5}{4\dot{m}}. \tag{33}$$

LEAKAGE FLOW THROUGH LABYRINTH SEAL:

Lüdtke [23] has given an expression to estimate the leakage flow through a labyrinth seal which is generally used within centrifugal compressor. The expression can be written as (replacing ideal gas assumption)

$$\dot{m}_{lk} = \zeta \cdot A \cdot \varepsilon \cdot \sqrt{p_{in}} \cdot \sqrt{\rho_{in}}. \tag{34}$$

where p_{in} and ρ_{in} represent the fluid pressure and density at the seal inlet respectively. The seal factor $\zeta \cdot A$ is not displayed in Hacks et al. [16]. However, it has been calculated by Hacks et al. through the experimental results of sCO2-HeRo in Hacks et al. [16] and has a value of 0.0009 for the compressor. The seal coefficient is estimated by Figure 9. The pressure ratio of the seal is obtained by assuming that the outlet pressure p_{out} of the seals is as same as the inlet pressure of the compressor.

In order to calculate the pressure at the seal inlet, the pressure drop in the disk/housing gap is calculated by the equations according to Aungier [4]:

$$\frac{\partial p}{\partial r} = K^2 \omega^2 \rho r \tag{35}$$

with

$$K = \frac{0.46}{1 + \frac{t}{r}} + \frac{\dot{m}_{lk} \cdot \left(\rho \cdot r_2 \cdot \frac{u_2}{\mu}\right)^{0.2}}{2\pi \cdot \rho \cdot r_2 \cdot u_2 \cdot t} \cdot \left(1.75 \cdot \frac{c_{u2}}{u_2} - 0.316\right). \tag{36}$$

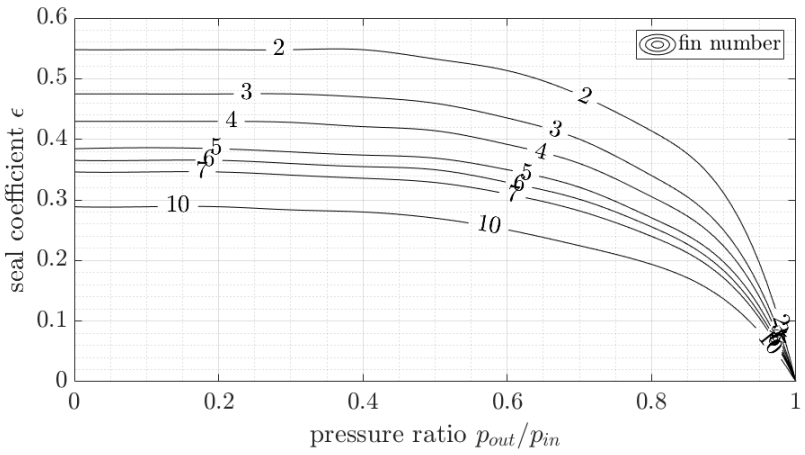

Figure 9: Seal coefficient according to Lüdtke [23]

FLOW ANGLES:

The flow angles defined in this paper are illustrated below:

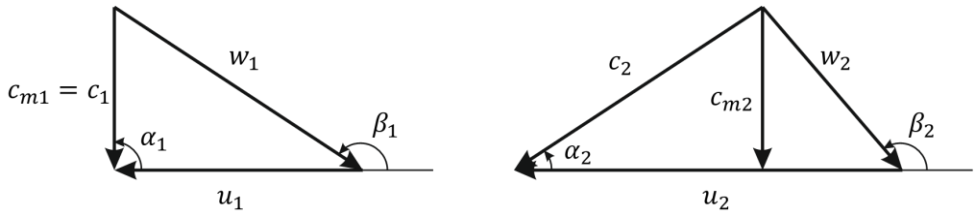

Figure 10: Velocity triangles at impeller inlet (left) and outlet (right)

DOI: 10.17185/duepublico/73948
URN: urn:nbn:de:hbz:464-20210330-093901-8